Scientia Iranica B (2022) 29(6), 3072–3083

Sharif University of Technology
Scientia Iranica
Transactions B: Mechanical Engineering
http://scientiairanica.sharif.edu

Theoretical study of two-dimensional unsteady Maxwell fluid flow over a vertical Riga plate under radiation effects

B. Ishtiaq[a,*], S. Nadeem[a], and N. Abbas[b]

a. *Department of Mathematics, Quaid-I-Azam University 45320, Islamabad 44000, Pakistan.*
b. *Department of Mathematics, Riphah International University, Faisalabad Campus, Faisalabad, 38000 Pakistan.*

Received 11 February 2022; received in revised form 11 May 2022; accepted 1 October 2022

KEYWORDS
Maxwell fluid;
Two-dimensional flow;
Thermal radiation;
Vertical Riga plate;
Unsteady flow;
Buongiorno model.

Abstract. The heat and mass transfer mechanism has gained importance in technical, industrial, and engineering processes following the use of thermal radiation in nanomaterials with improved thermal properties. Nanomaterials with improved thermal characteristics can be utilized in the formulation of energy to expand the industrial growth of countries. The effects of thermal radiation on the rate-type fluid passing through a Riga plate are examined in this article. The impact of thermophoresis and Brownian motion has significant importance. The mathematical explanation of the problem is given with the help of partial differential equations. The coupled nonlinear form of ordinary differential equations is achieved via the appropriate methodology of similarity variables. Utilizing suitable MATLAB software, we have achieved numerical solutions for simplified nonlinear equations. The physical parameters have exceptional impacts on the behavior of velocity, temperature, and concentration fields based on graphs. From this study, it is concluded that the Deborah number has an increasing effect on the pattern of fluid velocity. The rising values of the Prandtl number reduce the temperature profile while the higher values of the radiation parameter escalate the temperature profile.

1. Introduction

Today, research on non-Newtonian fluids has received considerable attention due to their rheological characteristics. There are various realistic implementations of these fluids in the industrial and engineering fields such as cooling systems, polymer extrusion, nuclear reactors, and food processing. All the features of these non-Newtonian fluids cannot be illustrated with the help of a single model. Thus, various non-Newtonian models have been introduced by a large number of researchers. The integral, rate-type, and differential fluids belong to the category of non-Newtonian models. The subclass of the rate-type fluid model includes Maxwell fluid. The Maxwell fluid characterizes the impact of relaxation time. Many studies are linked to Maxwell fluid (see [1–4]). Many researchers have been inspired by the available literature on non-Newtonian fluids to investigate the significant properties and behaviors of these fluid flows. Fetecau et al. [5] considered a continuously escalating plate and investigated the unsteady flow of generalized Maxwell fluid. Fetecau and Fetecau [6] studied the Maxwell fluid flow phenomenon caused by an infinite plate and obtained the exact results. Hayat and Qasim [7] conducted a study to explore the consequences of Joule heating and thermophoresis on the Magnetohydrodynamic (MHD)

*. *Corresponding author.*
E-mail address: bushraishtiaq@math.qau.edu.pk (B. Ishtiaq)

doi: 10.24200/sci.2022.59949.6514

Maxwell fluid flow. They obtained the series representation of the flow problem and concluded that the radiation parameter lowered the heat transfer rate. Jamil and Fetecau [8] considered coaxial cylinders to observe the Maxwell fluid for the Helical flow. They compared the Maxwell fluid flow mechanism with Newtonian fluids through graphs. Wang and Hayat [9] observed the fluctuating flow problem of Maxwell fluid in a porous medium by considering variable suction. Nadeem et al. [10] addressed the MHD boundary layer flow of Maxwell fluid exhibited by a stretching sheet subject to nanoparticles. They acquired the numerical results of the flow problem with the consideration of nanoparticles. Oke and Mutuku [11] considered a convectively heated stretchable sheet to examine the time-independent hydromagnetic boundary layer flow mechanism with viscous dissipation effects in Eyring-Powell fluid. The consequence of thermal radiation and Coriolis forces on MHD flow of modified Eyring-Powell fluid induced by a non-uniform surface was demonstrated by Oke [12]. The flow problem of water-Alumina nanofluid past on a uniform surface subject to the heat source and Coriolis effects was disclosed by Oke et al. [13]. The significance of thermal radiation in Williamson fluid subject to the hydromagnetic stagnation point flow past on a stretching sheet was analyzed by Ouru et al. [14]. Oyem et al. [15] investigated the time-independent MHD flow phenomenon initiated by a flat plate in the presence of Soret and Dufour in Sakiadis and Blasius flows. Sadeghy et al. [16] carried out a study to ensure a concise description of the upper-convected Maxwell (UCM) fluid past on a stationary plate. Hayat et al. [17] carried out the analysis of Maxwell fluid in ferromagnetic flow produced by a stretching sheet. Hayat et al. [18] also investigated the Cross fluid for MHD stagnation point flow and heat transfer phenomenon by taking into account a stretching surface. They concluded that the Prandtl number diminished the temperature distribution and the Weissenberg number enhanced the velocity distribution. Khan et al. [19] developed a study on non-Newtonian fluid in the magneto-nanomaterial flow to examine the heat transport mechanism and entropy optimization by considering a stretching curved surface. Khan et al. [20] considered a Darcy-Forchheimer porous medium to analyze the micropolar ferrofluid in the flow of second-order velocity slip.

The heat transfer mechanism and MHD flow of UCM fluid corresponding to a stretching surface with the consideration of thermal radiation were discovered by Abel et al. [21]. Mukhopadhyay et al. [22] considered a constantly permeable growing surface to detail the thermal radiation impacts on the Maxwell fluid. They observed the different characteristics of fluid flow and heat transfer. Zheng et al. [23] achieved accurate results for the problem of generalized Maxwell coaxial cylinders in an unsteady rotating flow. Hafeez et al. [24] considered a shrinking surface to observe the buoyancy impact on Cross nanofluid in chemically reactive flow. They studied the dual solutions to the problem and determined that the dual results existed in the range of critical points. Yang et al. [25] presented an article on the Casson nanofluid in MHD thermally radiative stagnation point flow constrained by a shrinking sheet. They utilized the Runge-Kutta Fehlberg methodology for the numerical outcomes and determined that the rate of heat transfer declined with the higher magnitude of the unsteadiness parameter. Khan et al. [26] investigated the cross nanofluid to discover the impact of thermal radiation on the stagnation point flow, passing through a shrinking surface. Hayat et al. [27] addressed the radiative nonlinear flow produced due to a convective cylinder and noticed that the magnetic and radiation parameters increased the temperature distribution. Qayyum et al. [28] established a brief study on five nanoparticles in the viscous fluid flow subject to a rotating disk with joule heating effects. The analysis of viscoelastic nanofluid for the radiative energy transmission with the appearance of convective conditions and buoyancy was executed by Waqas et al. [29]. The study of hybrid nanofluid for the MHD flow conducted by a rotating disk subject to entropy generation was carried out by Khan et al. [30]. The authors revealed that the extension of magnetic and stretching parameters improved the surface drag force. Gireesha et al. [31] discussed the mechanism of hybrid nanofluid flow developed by a moving permeable longitudinal fin and scrutinized the consequences of natural convection and thermal radiation. Hayat et al. [32] assumed pseudoplastic fluid in the presence of peristaltic flow to recognize the impacts of Joule heating, heat generation, Hall current, and Soret.

Riga plate was invented by Gailitis and Lielausis [33] to develop and work out the electric and magnetic fields, due to which Lorentz forces were established parallel to the wall to handle the fluid flow. Pantokratoras [34] used a Riga plate to demonstrate the Blasius and Sakiadis flows. The analysis of Blasius flow for an electrically conducting fluid with the existence of a Riga plate was carried out by Magyari and Pantokratoras [35]. Ahmad et al. [36] investigated the nanofluid for the mixed convective boundary layer flow induced by a Riga plate. The consequence of heat and mass transfer in the stagnation point flow phenomenon of the micropolar nanofluid subject to a Riga plate was scrutinized by Nadeem et al. [37]. The stagnation point flow phenomenon of Cosserat-Maxwell fluid with various physical impacts was analyzed by Hafeez et al. [38]. Fetecau et al. [39] studied a problem of flow between two parallel infinite plates to observe the exponential temperature-dependent viscosity of UCM fluid. Muhammad et al. [40] investigated the impacts of nonlinear thermal radiation and activation energy in Eyring-Powell nanofluid flow generated by a Riga plate. Waqas et al. [41] considered a stretchable cylinder to demonstrate the impacts of activation energy with heat and mass fluxes in the bio-convection Darcy-Forchheimer flow phenomenon of nanofluid. Zhang et al. [42] studied a porous Riga plate to investigate the thermo-bioconvection and oxytactic microorganism flow of nanofluid. The MHD flow problem resulting from a stretchable sheet in Maxwell nanofluid with the consideration of carbon nanotubes was analyzed by Subbarayudu et al. [43]. The phenomenon of bioconvection in Maxwell nanofluid flow caused by a Riga surface with the involvement of nonlinear thermal radiation and the activation energy was disclosed by Ramesh et al. [44].

According to the above-mentioned literature review, the Maxwell fluid flow problem over a Riga plate has been studied, while the time-dependent flow of Maxwell fluid over a vertical Riga plate with the existence of thermal radiation effects and the Buongiorno model has not been examined yet.

As part of its novelty, this study reports two-dimensional unsteady Maxwell fluid flow on a vertical Riga plate under radiation effects. To formulate the mathematical expressions of the physical problem, the Buongiorno model is considered. After the implementation of the relevant similarity transformations on the mathematical formulation of the problem, nonlinear coupled ordinary differential equations are acquired. To achieve numerical solutions of nonlinear ODEs, MATLAB package along with its bvp4c technique was employed. The impact of various parameters on the pattern of concentration, velocity, and temperature fields is determined through graphical presentations. The mathematical forms of the Sherwood number and local Nusselt number are determined.

2. Mathematical description

To examine the thermal radiation effects, let us take a vertical Riga plate with velocity U_w for the unsteady two-dimensional Maxwell fluid flow. The mathematical illustration of the problem considers the Buongiorno model, which incorporates the Brownian motion and thermophoresis effects. To understand the physical phenomena of the present problem, it is important to arrange the Cartesian coordinates system such that along the vertical Riga plate, the x-axis is taken and the y-axis direction is located orthogonally. The physical explanation of the ongoing flow problem is depicted in Figure 1.

We have the following relevant boundary layer equations for the given problem based on the above assumptions [45]:

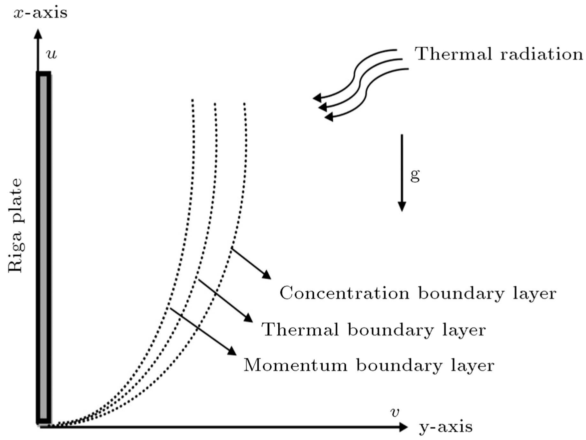

Figure 1. Physical description of the problem.

$$u_x + \nu_y = 0, \tag{1}$$

$$\begin{aligned}(u_t + uu_x + \nu u_y) &= \upsilon u_{yy} \\ &+\lambda(u^2 u_{xx} + \nu^2 u_{yy} + 2u\nu u_{xy}) \\ &+\frac{\pi M_0 j_0}{8\rho}\exp\left(-\frac{\pi}{b}y\right) + \frac{g\beta_T}{\rho}(T - T_\infty) \\ &+\frac{g\beta_C}{\rho}(C - C_\infty),\end{aligned} \tag{2}$$

$$\begin{aligned}\rho C_p(T_t + uT_x + \nu T_y) &= KT_{yy} + \mu(u_y)^2 - q_{r\,y} \\ &+\tau\left(D_B T_y C_y + \frac{D_T}{T_\infty}(T_y)^2\right),\end{aligned} \tag{3}$$

$$(C_t + uC_x + \nu C_y) = D_B(C_{yy}) + \frac{D_T}{T_\infty}(T_{yy}). \tag{4}$$

In Eq. (3), the radiative heat flux has the following expression as described by Eckert et al. [46] and Raptis [47]:

$$q_r = -\frac{4\sigma^*}{3k_1}\frac{\partial T^4}{\partial y}. \tag{5}$$

Following the application of the expansion $T^4 \cong 4T_\infty^3 T - 3T_\infty^4$, Eq. (3) takes the following form:

$$\begin{aligned}\rho C_p(T_t + uT_x + \nu T_y) &= \left(K + \frac{16\sigma^* T_\infty^3}{3k_1}\right)T_{yy} \\ &+\mu(u_y)^2 + \tau\left(D_B T_y C_y + \frac{D_T}{T_\infty}(T_y)^2\right).\end{aligned} \tag{6}$$

The relevant boundary conditions for the concerned problem are defined as follows:

$$u = U_w(x,t) = \frac{x}{1-ct},$$

$$\nu = V_w(x,t) = -\frac{\nu_o}{(1-ct)^{1/2}},$$

$$T = T_w(x,t) = T_\infty + T_o\frac{ax}{2v(1-ct)^2},$$

$$D_B C_y + \frac{D_T}{T_\infty}T_y, \qquad \text{at} \quad y=0,$$

$$u \to 0, \quad T \to T_\infty, \quad C \to C_\infty \quad \text{as} \quad y \to \infty, \tag{7}$$

where U_w is the surface velocity and V_m is mass flux velocity with $V_w \prec 0$ for injection and $V_w \succ 0$ for suction and constants $a \succ 0$, $c \geq 0 (ct \prec 1)$.

The relevant similarity variables are defined as follows [45]:

$$\psi = \sqrt{vxU_w}f(\eta), \qquad \theta(\eta) = \frac{T-T_\infty}{T_w-T_\infty},$$

$$\phi(\eta) = \frac{C-C_\infty}{C_w-C_\infty}, \qquad \eta = \sqrt{\frac{U_w}{xv}}y,$$

$$u = \psi_y, \qquad \nu = -\psi_x. \tag{8}$$

The following non-linear equations are obtained upon using Eqs. (2), (4), (6), and (8):

$$f''' + ff'' - f'^2 - S\left(\frac{1}{2}\eta f'' + f'\right) + \beta(f^2 f''' - 2ff'f'')$$
$$+ M\exp(-\xi\eta) + Gr\theta + Gc\phi = 0, \tag{9}$$

$$\left(1+\frac{4}{3}Rd\right)\theta'' + PrEcf''^2 - Pr\left(\frac{S}{2}\eta\theta' - f\theta'\right)$$
$$+ PrNb\theta'\phi' + PrNt\theta'^2 = 0, \tag{10}$$

$$\phi'' + \frac{Nt}{Nb}\theta'' + Scf\phi' - Sc\frac{S}{2}\eta\phi' = 0. \tag{11}$$

Eq. (7) takes the form:

$$f(0) = A, \quad f'(0) = 1, \qquad \theta(0) = 1,$$

$$Nb\phi'(0) + Nt\theta'(0) = 0, \qquad f'(\infty) = 0,$$

$$\theta(\infty) = 0, \qquad \phi(\infty) = 0. \tag{12}$$

Here, we have:

$$S = \frac{c}{a}, \quad \beta = \frac{\lambda U_w}{x}, \quad M = \frac{\pi M_0 j_0}{8\rho}\frac{x}{U_w^2},$$

$$Gr = \frac{x}{U_w^2}\frac{g\beta_T}{\rho}(T_w - T_\infty), \quad Gc = \frac{x}{U_w^2}\frac{g\beta_C}{\rho}(C_w - C_\infty),$$

$$Sc = \frac{v}{D_B}, \quad \xi = \frac{\pi}{b}\sqrt{\frac{vx}{U_w}}, \quad Rd = \frac{4\sigma^* T_\infty^3}{k_1 K}, \quad Pr = \frac{\mu C_p}{K},$$

$$Ec = \frac{U_w^2}{C_p(T_w - T_\infty)}, \quad Nb = \frac{\tau D_B(C_w - C_\infty)}{v},$$

$$Nt = \frac{\tau D_T(T_w - T_\infty)}{vT_\infty}, \quad A = \frac{v_0}{\sqrt{av}}. \tag{13}$$

Local Nusselt and Sherwood numbers are stated mathematically as [48]:

$$Nu_x = \frac{xq_w}{K(T_w - T_\infty)}, \qquad Sh_x = \frac{xh_m}{D_B(C_w - C_\infty)},$$

$$q_w = -K\left(1 + \frac{16\sigma^* T_\infty^3}{3k_1 K}\right)\left(\frac{\partial T}{\partial y}\right)_{y=0},$$

$$h_m = -D_B\left(\frac{\partial C}{\partial y}\right)_{y=0},$$

$$Re_x^{-1/2}Nu_x = -\left(1+\frac{4}{3}Rd\right)\theta'(0),$$

$$Re_x^{-1/2}Sh_x = -\phi'(0). \tag{14}$$

3. Solution procedure

To solve the nonlinear higher-order ODEs, we will first convert them into the first-order problem. To this end, the numerical technique outlined below is employed. Eqs. (9)–(11) can be rewritten as follows:

$$f''' = \left(\frac{1}{1+\beta f^2}\right)\left(S\left(\frac{1}{2}\eta f'' + f'\right) + f'^2 - ff''\right.$$
$$\left. + 2\beta ff'f'' - M\exp(-\xi\eta) - Gr\theta - Gc\phi\right), \tag{15}$$

$$\theta'' = \left(\frac{1}{1+\frac{4}{3}Rd}\right)\left(Pr\left(\frac{S}{2}\eta\theta' - f\theta'\right) - PrEcf''^2\right.$$
$$\left. - PrNb\theta'\phi' - PrNt\theta'^2\right), \tag{16}$$

$$\phi'' = Sc\frac{S}{2}\eta\phi' - \frac{Nt}{Nb}\theta'' - Scf\phi'. \tag{17}$$

Now, to transform the above higher-order ODEs into the system of the first order, seven new variables are developed. Eqs. (15)–(17) are of order three in f and order two in θ and ϕ, respectively. The new variables are introduced as follows:

$$f = y_1, \quad f' = y_2, \quad f'' = y_3, \quad f''' = y_3',$$

$$\theta = y_4, \quad \theta' = y_5, \quad \theta'' = y_5',$$

$$\phi = y_6, \quad \phi' = y_7, \quad \phi'' = y_7'. \tag{18}$$

We have the following first-order system of equations after substituting Eq. (18) into Eqs. (15)–(17).

$$y_2 = y_1', \qquad y_3 = y_2', \tag{19}$$

$$y_3' = \frac{1}{1+\beta y_1^2}\left[S\left(\frac{1}{2}\eta y_3 + y_2\right) + y_2^2 - y_1 y_3 + 2\beta y_1 y_2 y_3 - M\exp(-\xi\eta) - Gr y_4 - Gc y_6\right],$$

$$y_5 = y_4', \tag{20}$$

$$y_5' = \frac{1}{1+\frac{4}{3}Rd}\left[Pr\left(\frac{S}{2}\eta y_5 - y_1 y_5\right) - PrEc y_3^2 - PrNb y_5 y_7 - PrNt y_5^2\right],$$

$$y_7 = y_6', \qquad y_7' = Sc\frac{S}{2}\eta y_7 - \frac{Nt}{Nb}y_5' - Sc y_1 y_7. \tag{21}$$

The boundary conditions (12) take the following form in the new variables:

$$y_0(1) = A, \quad y_0(2) = 1, \quad y_0(4) = 1,$$

$$Nb y_0(7) + Nt y_0(5) = 0,$$

$$y_\infty(2) = 0, \quad y_\infty(4) = 0, \quad y_\infty(6) = 0. \tag{22}$$

4. Results and discussion

The solution to Eqs. (9)–(11) subject to Eq. (12) was obtained using MATLAB software by its bvp4c methodology. Graphs employed to examine the influence of numerous parameters appearing in equations on dimensionless velocity, temperature, and concentration were sketched. A range of relevant parameters include $\beta = 0.2, S = 0.5, C = 0.5, M = 0.1, N = 0.4, Rd = 1.2, \Pr = 1.5, Ec = 0.8, Nb = 0.2, Nt = 0.7, Sc = 1.3, A = 0.9$, and $V = 0.2$. Figure 2 is sketched to examine the behavior of the velocity curve with the proceeding values of the Deborah number. Physically, the Deborah number is related to the relaxation time; therefore, due to the melting phenomenon, the higher values of β show lower viscous force to the fluid particle motion and the velocity curve exhibits an escalating behavior. For expanding the parameters S, Sc, and A the dimensionless velocity curve declines, as shown in Figures 3–5. The pattern of dimensionless velocity exhibits the declining behavior due to the diminishing thickness of the momentum boundary layer with the escalating value of S. In the case of $S = 0$ we have a steady flow and an unsteady flow for $S \succ 0$. The fluid velocity descends due to the greater intensity of SC, as displayed in Figure 4. Physically, with increase in the value of Sc the viscous effect is escalated due to which the velocity of fluid declines. According to Figure 5, with acceleration in the magnitude of A, the boundary layer thickness shrinks; therefore, there is a decrement in the fluid velocity. The impacts of parameters Pr, Rd, S, Ec, Nb, and Nt on the temperature field are depicted in Figures 6–11. Figure 6 is sketched to explain the behavior of temperature distribution for Pr The accelerating values of Pr reduce the thickness of the boundary layer and decline the temperature curve. The momentum diffusion becomes superior and the thermal boundary layer goes thin, thus reducing the temperature profile. The higher increment in the Prandtl number reduces the fluid thermal conductivity. As a result, the heat transfer decelerates, thus lowering the fluid temperature. Figures 7 and 8 show that the magnitude of the temperature field rises due to increment in parameters Rd and S, respectively. Phys-

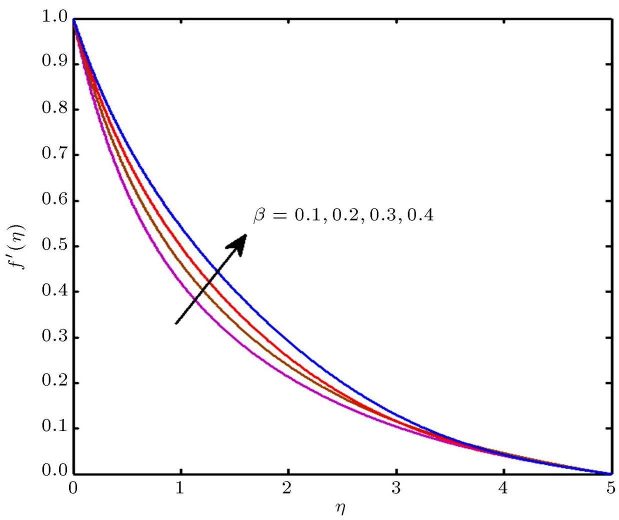

Figure 2. Velocity curve corresponding to the Deborah number.

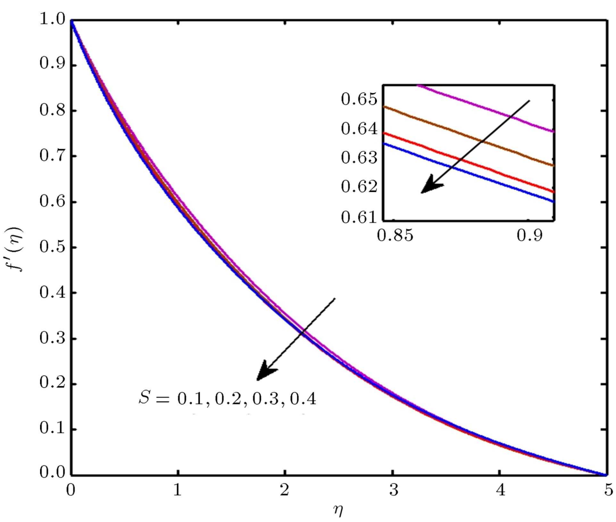

Figure 3. Velocity curve corresponding to the unsteadiness parameter.

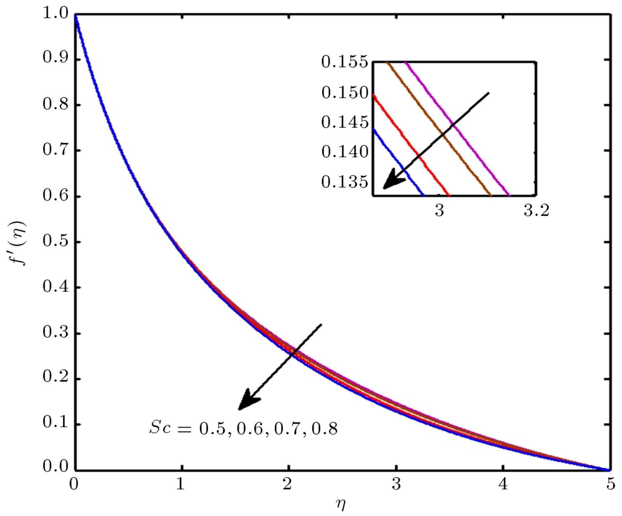

Figure 4. Velocity curve corresponding to the Schmidt number.

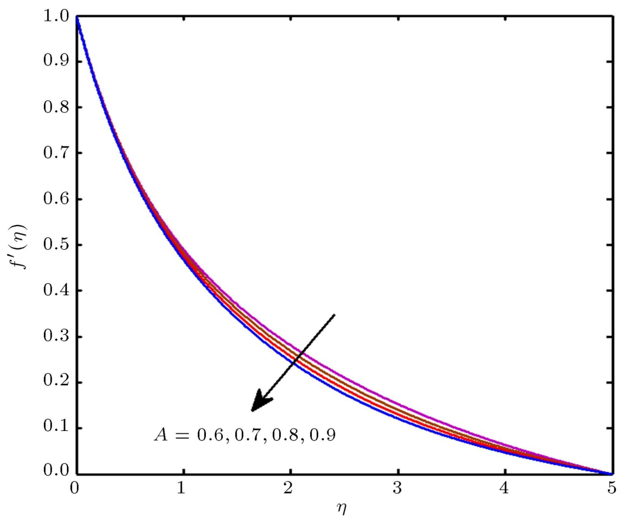

Figure 5. Velocity curve corresponding to the Suction parameter.

ically, the radiation parameter determines how much the conduction heat transfer yields thermal radiation transfer. We have come up with the result that the higher magnitude of Rd escalates the temperature profile within the boundary layer. The fluid internal energy and temperature field rise with an increase in the value of Ec, as depicted in Figure 9. The Eckert number is used to illustrate the relation between the kinetic energy of fluid flow and the heat enthalpy difference. The fluid temperature is also considered as the average kinetic energy, which is a familiar fact. Furthermore, the flow kinetic energy expands due to increase in the value of Ec parameter. As a result, the fluid temperature proceeds. Figure 10 illustrates the temperature field behavior with the effects of increasing the values of Nb. The fluid temperature field exhibits an expanding behavior at a higher magnitude of Nb. In

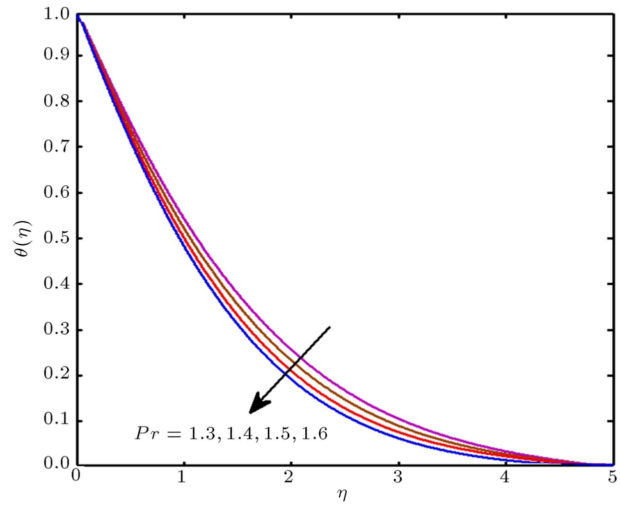

Figure 6. Temperature curve corresponding to the Prandtl number.

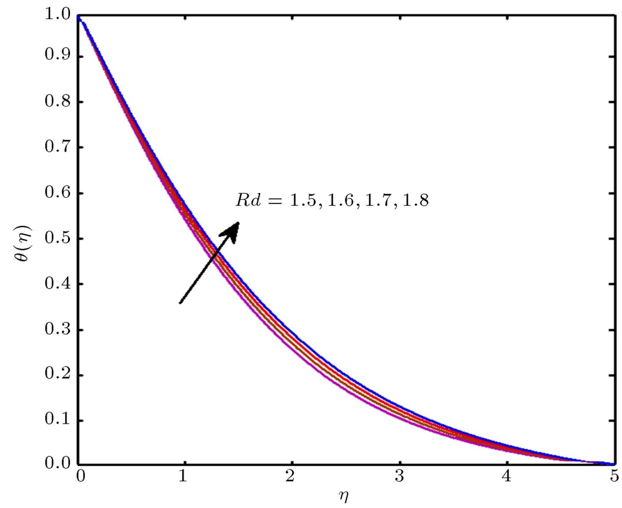

Figure 7. Temperature curve corresponding to the radiation parameter.

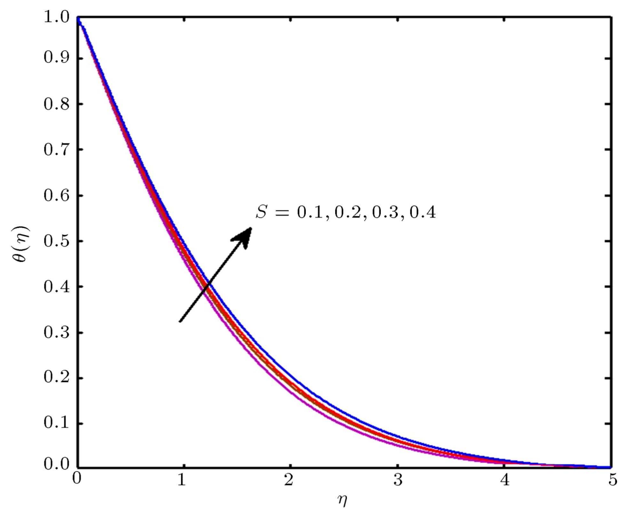

Figure 8. Temperature curve corresponding to the unsteadiness parameter.

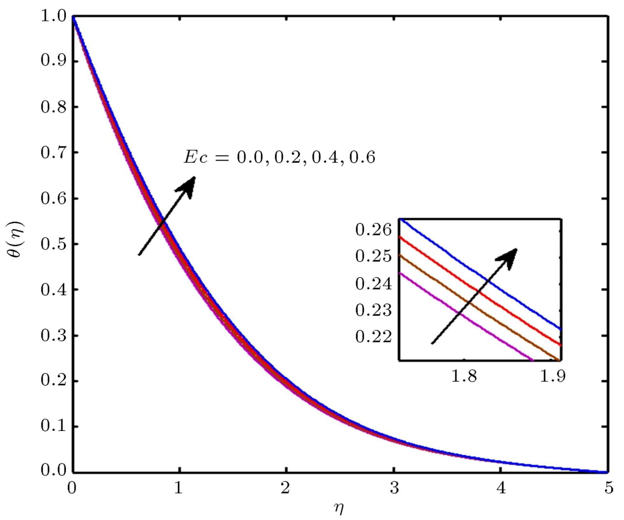

Figure 9. Temperature curve corresponding to the Eckert number.

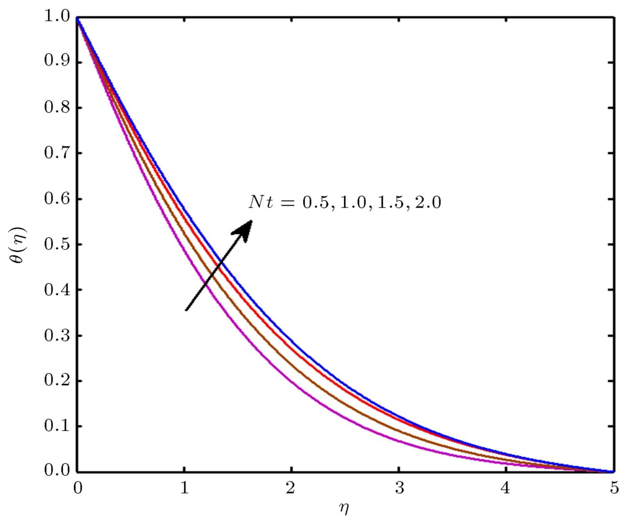

Figure 11. Temperature curve corresponding to the thermophoresis parameter.

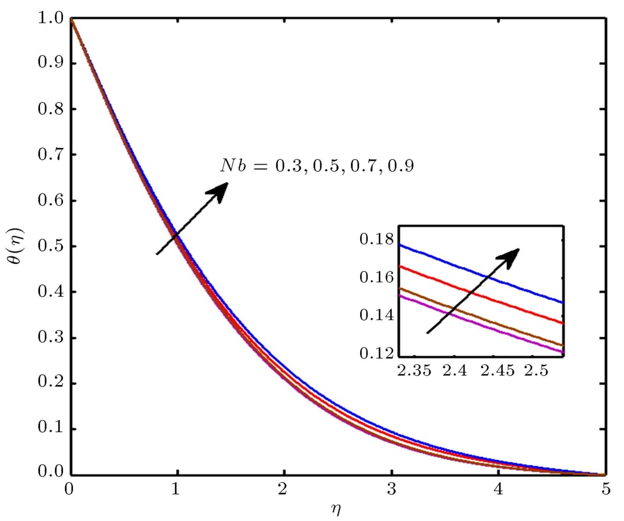

Figure 10. Temperature curve corresponding to the Brownian motion parameter.

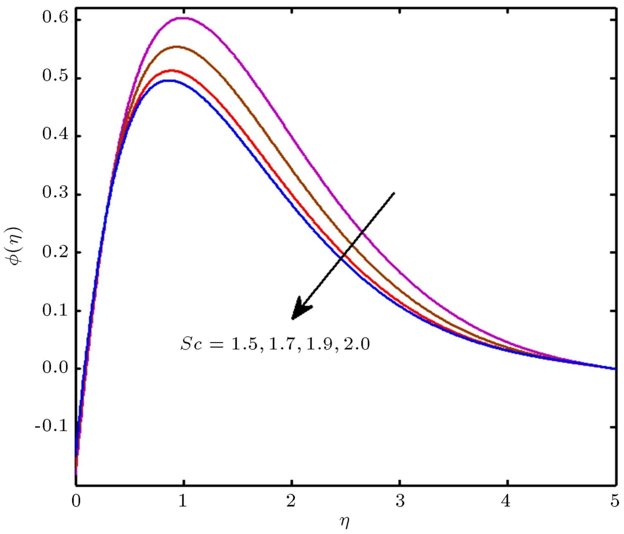

Figure 12. Concentration curve corresponding to the Schmidt number.

fluids, the arbitrary movement of nanoparticles results from the Brownian motion. The collision between nanoparticles and fluid molecules is enhanced due to this movement. As a result, the kinetic energy of molecules takes the form of thermal energy and therefore, fluid temperature increases. The behavior of fluid temperature for Nt is given in Figure 11. Physically, the motion of the particles from the hotter section to the cold section escalates due to thermophoresis. The temperature increases because of the quick motion of heat from a hotter surface to the fluid. Figure 12 examines the declining magnitude of the concentration field against Sc. As the Schmidt number is related to the Brownian diffusion coefficient, an increase in the Schmidt number lowers the Brownian coefficient. Moreover, the nanoparticles experience resistance in penetrating heavier into the fluid. As a result, as the Schmidt number escalates, the infiltration depth of concentration descends. In the case of the parameter S, concentration is an increasing function, as depicted in Figure 13. The concentration field declines with the growing Nb values, as exhibited in Figure 14. The rate of Brownian diffusion rises due to Brownian parameter and concentration field is reduced. The accelerating behavior of concentration due to Nt increase is explored in Figure 15. Physically, the thermophoretic diffusion is intensified at a higher magnitude of Nt. As a result, the nanoparticles move to the cool fluid from the hot region. Therefore, the higher values of Nt enhance the thickness of the concentration boundary layer.

For distinct values of Pr Table 1 presents excellent agreement between the obtained numerical values of the Nusselt number and those obtained by Nadeem et al. [49]. Table 2 shows the numerical values of

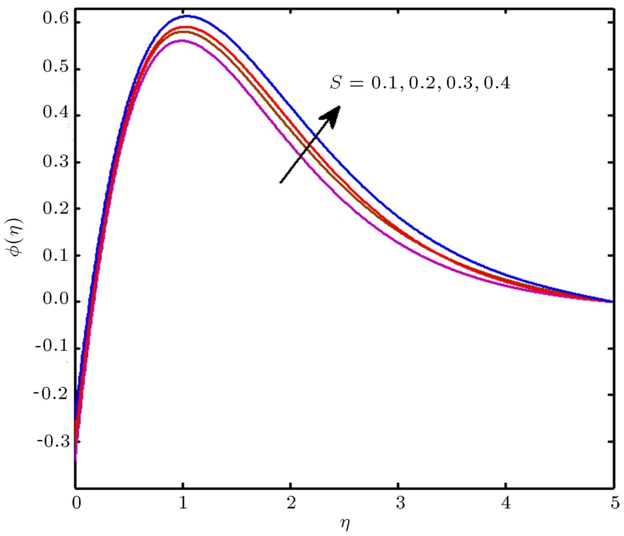

Figure 13. Concentration curve corresponding to the unsteadiness parameter.

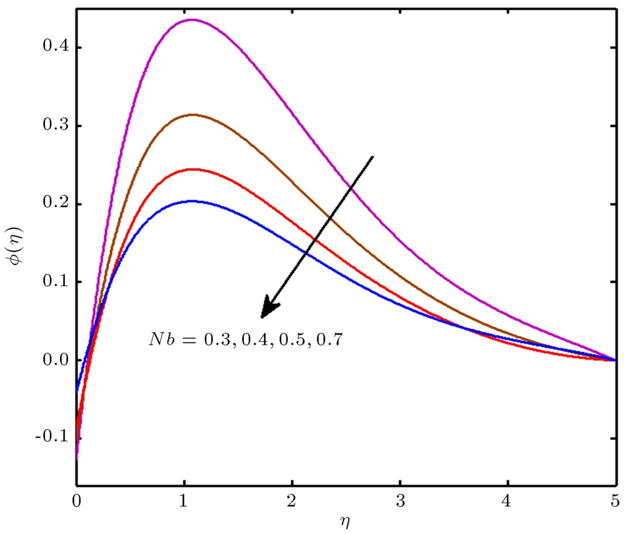

Figure 14. Concentration curve corresponding to the Brownian motion parameter.

the Nusselt number $\mathrm{Re}_x^{-1/2} Nu_x$ and Sherwood number $\mathrm{Re}_x^{-1/2} Sh_x$ corresponding to distinct values of physical parameters. The values of Nusselt number for S, Rd, Ec, Nt, and Sc are reduced, while values of β and Pr increase. At higher values of β, Pr, and Nt, the values of Sherwood number increase, exhibiting the opposite behavior for S, Pr, Rd, Ec, Nb, and Sc.

Table 1. Comparison of the Nusselt number with different values of Pr.

Pr	Present results	Nadeem et al. [49]
0.7	0.4582	0.4582
2.0	0.9114	0.9114
7.0	1.8955	1.8954
20	3.3539	3.3539
70	6.4621	6.4622

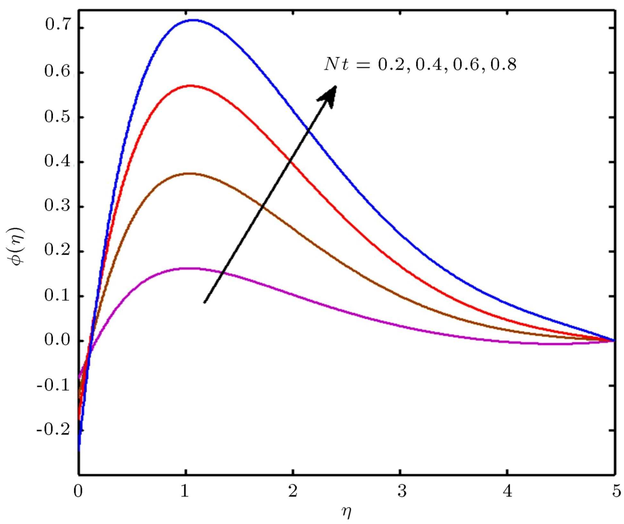

Figure 15. Concentration curve corresponding to the thermophoresis parameter.

5. Concluding remarks

The consequence of thermal radiation on the time-dependent two-dimensional flow of Maxwell fluid subject to a vertical Riga plate was briefly investigated in this paper. The Buongiorno model with the effects of Brownian motion and thermophoresis was also considered. With the help of MATLAB software along with its bvp4c methodology, the numerical outcomes of the nonlinear system of ODEs were achieved. Graphical presentations were used to examine the temperature, velocity, and concentration fields corresponding to the various pertinent parameters. The main findings of the concerned problem are exhibited below:

- The pattern of dimensionless velocity takes a descending pattern for parameters S, Sc, and A, while it depicts the increasing behavior at the escalating values of β. The thickness of the momentum boundary layer rises with the increment in β due to which the velocity field raises;
- Temperature field varies directly for Rd, S, Ec, Nb, and Nt, while it descents for Pr. The fluid thermal conductivity is reduced as the Pr values go upward. Furthermore, the rate of heat transfer is minimized, which reduces the temperature distribution;
- Concentration increases due to S and Nt;
- Impact of Sc and Nb for concentration is completely different from S and Nt. The concentration distribution takes a descending pattern at higher values of Sc and Nb;

Table 2. At distinct values of involving parameters, computational results of Nusselt number and Sherwood number.

β	S	Pr	Rd	Ec	Nb	Nt	Sc	$Re_x^{-1/2}Nu_x$	$Re_x^{-1/2}Sh_x$
0.3	0.5	1.5	1.2	0.8	0.2	0.7	1.3	1.6458	2.2155
0.4								1.7786	2.3943
0.5								2.0429	2.7501
0.6								2.4066	3.2396
0.5	0.1	1.5	1.2	0.8	0.2	0.7	1.3	1.6588	2.2331
	0.3							1.5576	2.0967
	0.5							1.4798	1.9921
	0.7							1.4127	1.9017
0.5	0.5	0.2	1.2	0.8	0.2	0.7	1.3	0.6067	0.8167
		0.4						0.7056	0.9498
		0.7						0.8834	1.1892
		0.8						0.9474	1.2753
0.5	0.5	1.5	0.1	0.8	0.2	0.7	1.3	2.6754	8.2621
			0.2					1.7336	4.7903
			0.3					1.5146	3.7866
			0.4					1.4402	3.2873
0.5	0.5	1.5	1.2	0.2	0.2	0.7	1.3	0.2266	0.7932
				0.3				0.2019	0.7068
				0.4				0.1773	0.6204
				0.5				0.1526	0.5340
0.5	0.5	1.5	1.2	0.8	0.1	0.7	1.3	0.0785	0.5495
					0.2			0.0785	0.2747
					0.3			0.0785	0.1831
					0.4			0.0785	0.1374
0.5	0.5	1.5	1.2	0.8	0.2	0.2		0.0947	0.0947
						0.3		0.0914	0.1371
						0.4		0.0881	0.1762
						0.5		0.0848	0.2121
0.5	0.5	1.5	1.2	0.8	0.2	0.7	0.1	0.0987	0.3455
							0.2	0.0961	0.3364
							0.3	0.0937	0.3281
							0.4	0.0916	0.3205

- Nusselt number and Sherwood numbers have escalating values for β and Pr, but they are reduced for S, Rd, Ec, and Sc.

Nomenclature

u, v	Velocity components
x, y	Cartesian coordinates
g	Gravitational acceleration
v	Kinematic viscosity
M_0	Magnet magnetization
j_0	Applied current density
b	Electrodes and magnets width
K	Fluid thermal conductivity
ρ	Fluid density
β	Deborah number
T	Fluid temperature
T_∞	Ambient temperature
T_w	Temperature at the surface
C_∞	Ambient concentration
C_w	Surface concentration
η	Similarity variable
Sc	Schmidt number
h_m	Surface mass flux
θ	Dimensionless temperature
M	Modified Hartmann number
Gc	Modified Grashof number
σ^*	Stefan-Boltzmann constant
k_1	Mean absorption coefficient
S	Unsteadiness parameter
Pr	Prandtl number
Rd	Radiation parameter
ξ	Dimensionless parameter
Ec	Eckert number
Nt	Thermophoresis motion parameter
Nb	Brownian parameter
μ	Dynamic viscosity
q_r	Radiative heat flux
λ	Relaxation time
D_B	Brownian diffusion coefficient
D_T	Thermal diffusion coefficient
ψ	Stream function
c_p	Specific heat capacity at constant pressure
A	Suction parameter
q_w	Surface heat flux
ϕ	Dimensionless concentration
Gr	Local Grashof number

References

1. Khan, M.I., Waqas, M., Hayat, T., et al. "Behavior of stratification phenomenon in flow of Maxwell nanomaterial with motile gyrotactic microorganisms in the presence of magnetic field", *Int. J. Mech. Sci.,* **131**, pp. 426–434 (2017).

2. Zheng, L., Zhao, F., and Zhang, X. "Exact solutions for generalized Maxwell fluid flow due to oscillatory and constantly accelerating plate", *Nonlinear Anal. Real World Appl.*, **11**(5), pp. 3744–3751 (2010).

3. Khan, M.I., Khan, M.I., Waqas, M., et al. "Chemically reactive flow of Maxwell liquid due to variable thicked surface", *Int. Commun. Heat Mass Transf.*, **86**, pp. 231–238 (2017).

4. Abbas, Z., Sajid, M., and Hayat, T. "MHD boundary-layer flow of an upper-convected Maxwell fluid in a porous channel", *Theor Comput Fluid Dyn*, **20**(4), pp. 229–238 (2006).

5. Fetecau, C., Athar, M., and Fetecau, C. "Unsteady flow of a generalized Maxwell fluid with fractional derivative due to a constantly accelerating plate", *Comput. Math. Appl.*, **57**(4), pp. 596–603 (2009).

6. Fetecau, C. and Fetecau, C. "A new exact solution for the flow of a Maxwell fluid past an infinite plate", *Int. J. Non-Linear Mech.*, **38**(3), pp. 423–427 (2003).

7. Hayat, T. and Qasim, M. "Influence of thermal radiation and Joule heating on MHD flow of a Maxwell fluid in the presence of thermophoresis", *Int. J. Heat Mass Transf.*, **53**(21–22), pp. 4780–4788 (2010).

8. Jamil, M. and Fetecau, C. "Helical flows of Maxwell fluid between coaxial cylinders with given shear stresses on the boundary", *Nonlinear Anal. Real World Appl.*, **11**(5), pp. 4302–4311 (2010).

9. Wang, Y. and Hayat, T. "Fluctuating flow of a Maxwell fluid past a porous plate with variable suction", *Nonlinear Anal. Real World Appl.*, **9**(4), pp. 1269–1282 (2008).

10. Nadeem, S., Haq, R.U., and Khan, Z.H. "Numerical study of MHD boundary layer flow of a Maxwell fluid past a stretching sheet in the presence of nanoparticles", *J. Taiwan Inst Chem Eng*, **45**(1), pp. 121–126 (2014).

11. Oke, A.S. and Mutuku, W.N. "Significance of viscous dissipation on MHD Eyring-Powell flow past a convectively heated stretching sheet", *Pramana*, **95**(4), pp. 1–7 (2021).

12. Oke, A.S. "Coriolis effects on MHD flow of MEP fluid over a non-uniform surface in the presence of thermal radiation", *Int. Commun. Heat Mass Transf.*, **129**, 105695 (2021).

13. Oke, A.S., Animasaun, I.L., Mutuku, W.N., et al. "Significance of Coriolis force, volume fraction, and heat source/sink on the dynamics of water conveying 47 nm alumina nanoparticles over a uniform surface", *Chinese J. Phys.*, **71**, pp. 716–727 (2021).

14. Ouru, J.O., Mutuku, W.N., and Oke, A.S. "Buoyancy-induced MHD stagnation point flow of Williamson fluid with thermal radiation", *J. Eng. Res. Reports.*, **11**(4), pp. 9–18 (2020).

15. Oyem, A.O., Mutuku, W.N., and Oke, A.S. "Variability effects on magnetohydrodynamic for Blasius and Sakiadis flows in the presence of Dufour and Soret about a flat plate", *Engineering Reports*, **2**(10), e12249 (2020).

16. Sadeghy, K., Najafi, A.H., and Saffaripour, M. "Sakiadis flow of an upper-convected maxwell fluid", *Int. J. Non-Linear Mech.*, **40**, pp. 1220–1228 (2015).

17. Hayat, T., Ahmad, S., Khan, M.I., et al. "Simulation of ferromagnetic nanomaterial flow of Maxwell fluid", *Results Phys.*, **8**, pp. 34–40 (2018).

18. Hayat, T., Khan, M.I., Tamoor, M., et al. "Numerical simulation of heat transfer in MHD stagnation point flow of Cross fluid model towards a stretched surface", *Results Phys.*, **7**, pp. 1824–1827 (2017).

19. Khan, M.I. and Alzahrani, F. "Binary chemical reaction with activation energy in dissipative flow of non-Newtonian nanomaterial", *J. Theor Comput Chem*, **19**(03), p. 2040006 (2020).

20. Khan, M.I., Alzahrani, F., and Hobiny, A. "Simulation and modeling of second order velocity slip flow of micropolar ferrofluid with Darcy-Forchheimer porous medium", *J. Mater. Res. Technol.*, **9**(4), pp. 7335–7340 (2020).

21. Abel, M.S., Tawade, J.V., and Shinde, J.N. "The effects of MHD flow and heat transfer for the UCM fluid over a stretching surface in presence of thermal radiation", *Adv. Math. Phys.*, **2012**, pp. 1–21, Article ID 702681 (2012).

22. Mukhopadhyay, S., Ranjan De, P., and Layek, G.C. "Heat transfer characteristics for the Maxwell fluid flow past an unsteady stretching permeable surface embedded in a porous medium with thermal radiation", *J. Appl. Mech. Tech. Phys.*, **54**(3), pp. 385–396 (2013).

23. Zheng, L., Li, C., Zhang, X., et al. "Exact solutions for the unsteady rotating flows of a generalized Maxwell fluid with oscillating pressure gradient between coaxial cylinders", *Comput. Math. Appl.*, **62**(3), pp. 1105–1115 (2011).

24. Hafeez, A., Yasir, M., Khan, M., et al. "Buoyancy effect on the chemically reactive flow of Cross nanofluid over a shrinking surface: Dual solution", *Int. Commun. Heat Mass Transf.*, **126**, 105438 (2021).

25. Yang, D., Yasir, M., and Hamid, A. "Thermal transport analysis in stagnation-point flow of Casson nanofluid over a shrinking surface with viscous dissipation", *Waves in Random and Complex Media*, pp. 1–15 (2021).

26. Khan, M., Ahmad, L., Yasir, M., et al. "Numerical analysis in thermally radiative stagnation point flow of Cross nanofluid due to shrinking surface: dual solutions", *Appl. Nanosci.*, pp. 1–12 (2021).

27. Hayat, T., Tamoor, M., Khan, M.I., et al. "Numerical simulation for nonlinear radiative flow by convective cylinder", *Results Phys.*, **6**, pp. 1031–1035 (2016).

28. Qayyum, S., Khan, M.I., Hayat, T., et al. "Comparative investigation of five nanoparticles in flow of viscous fluid with Joule heating and slip due to rotating disk", *Physica B Condens.*, **534**, pp. 173–183 (2018).

29. Waqas, M., Khan, M.I., Hayat, T., et al. "Transportation of radiative energy in viscoelastic nanofluid considering buoyancy forces and convective conditions", *Chaos Solitons Fractals*, **130**, 109415 (2020).

30. Ijaz Khan, M., Alsaedi, A., Hayat, T., et al. "Modeling and computational analysis of hybrid class nanomaterials subject to entropy generation", *Comput Methods Programs Biomed*, **179**, p. 104973 (2019).

31. Gireesha, B.J., Sowmya, G., Khan, M.I., et al. "Flow of hybrid nanofluid across a permeable longitudinal moving fin along with thermal radiation and natural convection", *Comput Methods Programs Biomed*, **185**, 105166 (2020).

32. Hayat, T., Aslam, N., Khan, M.I., et al. "Physical significance of heat generation/absorption and Soret effects on peristalsis flow of pseudoplastic fluid in an inclined channel", *J. Mol. Liq.*, **275**, pp. 599–615 (2019).

33. Gailitis, A. "On the possibility to reduce the hydrodynamic drag of a plate in an electrolyte", *Appl. Magnetohydrodynamics, Rep. Inst. Phys. Riga*, **13**, pp. 143–146 (1961).

34. Pantokratoras, A. "The Blasius and Sakiadis flow along a Riga-plate", *Prog. Comput. Fluid Dyn.*, **11**(5), pp. 329–333 (2011).

35. Magyari, E. and Pantokratoras, A. "Aiding and opposing mixed convection flows over the Riga-plate", *Commun. Nonlinear Sci. Numer. Simul.*, **16**(8), pp. 3158–3167 (2011).

36. Ahmad, A., Asghar, S., and Afzal, S. "Flow of nanofluid past a Riga plate", *J. Magn. Magn. Mater.*, **402**, pp. 44–48 (2016).

37. Nadeem, S., Amin, A., Abbas, N., et al. "Effects of heat and mass transfer on stagnation point flow of micropolar Maxwell fluid over Riga plate", *Sci. Iran.*, **28**(6), pp. 3753–3766 (2021).

38. Hafeez, M.B., Khan, M.S., Qureshi, I.H., et al. "Particle rotation effects in Cosserat-Maxwell boundary layer flow with non-Fourier heat transfer using a new novel approach", *Sci. Iran.*, **28**(3), pp. 1223–1235 (2021).

39. Fetecau, C., Vieru, D., Abbas, T., et al. "Analytical solutions of upper convected Maxwell fluid with exponential dependence of viscosity under the influence of pressure", *Mathematics*, **9**(4), p. 334 (2021).

40. Muhammad, T., Waqas, H., Khan, S.A., et al. "Significance of nonlinear thermal radiation in 3D Eyring-Powell nanofluid flow with Arrhenius activation energy", *J. Therm. Anal. Calorim.*, **143**(2), pp. 929–944 (2021).

41. Waqas, H., Imran, M., Muhammad, T., et al. "On bio-convection thermal radiation in Darcy-Forchheimer flow of nanofluid with gyrotactic motile microorganism under Wu's slip over stretching cylinder/plate", *Int. J. Numer. Methods Heat Fluid Flow*, **31**, pp. 1520–1546 (2020).

42. Zhang, L., Bhatti, M.M., Ellahi, R., et al. "Oxytactic microorganisms and thermo-bioconvection nanofluid flow over a porous Riga plate with Darcy-Brinkman-Forchheimer medium", *J. Non-Equilib. Thermodyn.*, **45**(3), pp. 257–268 (2020).

43. Subbarayudu, K., Suneetha, S., Bala Anki Reddy, P., et al. "Framing the activation energy and binary chemical reaction on CNT's with Cattaneo–hristov heat diffusion on Maxwell nanofluid in the presence of nonlinear thermal radiation", *Arab. J. Sci. Eng.*, **44**(12), pp. 10313–10325 (2019).

44. Ramesh, K., Khan, S.U., Jameel, M., et al. "Bioconvection assessment in Maxwell nanofluid configured by a Riga surface with nonlinear thermal radiation and activation energy", *Surfaces and Interfaces*, **21**, 100749 (2020).

45. Ramesh, G.K., Roopa, G.S., Gireesha, B.J., et al. "An electro-magneto-hydrodynamic flow Maxwell nanoliquid past a Riga plate: a numerical study", *J. Braz. Soc. Mech. Sci. Eng.*, **39**(11), pp. 4547–4554 (2017).

46. Eckert, E.R.G., Sparrow, E.M., Goldstein, R.J., et al. "Heat transfer-A review of 1978 literature", *Int. J. Heat Mass Transf.*, **22**(11), pp. 1469–1499 (1979).

47. Raptis A. "Radiation and free convection flow through a porous medium", *Int. J. Heat Mass Transf.*, **25**(2), pp. 289–95 (1998).

48. Loganathan, K., Alessa, N., Namgyel, N., et al. "MHD flow of thermally radiative Maxwell fluid past a heated stretching sheet with Cattaneo-Christov dual diffusion", *J. Math.*, **2021**, Article ID 5562667, pp. 1–10 (2021).

49. Nadeem, S., Haq, R.U., and Khan, Z.H. "Numerical study of MHD boundary layer flow of a Maxwell fluid past a stretching sheet in the presence of nanoparticles", *J. Taiwan Inst Chem Eng*, **45**(1), pp. 121–126 (2014).

Biographies

Bushra Ishtiaq was born in Kamra, Punjab, Pakistan. She completed her MPhil degree from the Department of Mathematics at Quaid-i-Azam University, Islamabad, Pakistan and, currently, is PhD scholar at the Department of Mathematics, Quaid-I-Azam University 45320, Islamabad 44000, Pakistan. She published her work in international well-reputed impact-factor journals.

Sohail Nadeem is working as a Professor at the Department of Mathematics at Quaid-i-Azam University, Islamabad, Pakistan. More than 25 PhD scholars and more than 100 MPhil students have completed their respective degrees under his supervision. He has published more than 500 research articles in well-reputed international journals having more than 7000 citations. He has been awarded several national/international awards. He is also a member of several editorial boards in well-reputed international journals. Nationally, he is serving on several scientific committees throughout the country.

Nadeem Abbas was born on September 15, 1990, in District Jhang, Punjab, Pakistan. He earned his MSc degree in Mathematics in 2014 from the University of the Punjab Lahore, Pakistan and MPhil and PhD degrees from Quaid-i-Azam University Islamabad, Pakistan. Now, he is working as an Assistant Professor at the Department of Mathematics, Riphah International University, Faisalabad Campus, Pakistan. He has published more than 30 research articles in well-reputed international journals, having more than 470 citations.